Modeling and Numerical Investigations in the Behavior of One-dimensional Bubbly Cavitating Flows Through a Venturi

M. ZAMOUM[a], R. BOUCETTA[a], M. KESSAL[a]

a. Laboratoire Génie Physique des Hydrocarbures LGPH, Faculté des Hydrocarbures et de la Chimie FHC, Université M'hamed Bougara de Boumerdès, 35000, Algérie
m_zamoum2000@yahoo.fr

Abstract :

The research refers to the numerical study of cavitation phenomena when liquid-gas flow was passing through the venturi nozzle. The dynamics of the cavitating bubbles are modeled by the use of the mass and momentum phase's equations, which are coupled with the Rayleigh-Plesset equation of the N bubbles dynamics. However, assuming that the same initial conditions of all bubbles are identical and that all bubbles are equi-distant from each other simplifies the governing equations. The effects of the bubble population size and the upstream void fraction on flow parameters are investigated. The numerical resolution of the previous equations set (ODE) let us found that the bubble radius change dramatically with upstream void fraction and An instability appeared just after the throat of the Venturi for both cases one bubble (N=1) and two bubbles (N=2). Indeed, for the case of one bubble, the instability occurs for an upstream void fraction $\alpha_s=5.37 \times 10^{-3}$, which corresponds to a critical bubble radius $r_c=4$. Whereas, for bubble number N=2, the same phenomenon occurs for $\alpha_s = 1,344 \times 10^{-1}$, with $R_c=1.5$. Also, obtained numerical result shown that, as the number of bubbles is increased, the natural frequency and the damping of the bubbles decrease. Beside, the distance between bubbles decrease leads to increase of the damping and the natural frequency.

Keywords: Cavitating, Venturi, Bubbly flow

NOMENCLATURE

A　dimensionless cross-sectional area of the Venturi, A^*/A_s^*	R　dimensionless bubble radius, R^*/R_s^*
A*　cross-sectional area of the Venturi	R_c　dimensionless critical bubble radius at which flashing flow occurs
A_s^*　upstream cross-sectional area of the Venturi	R_s^*　upstream bubble radius
Cp　fluid pressure coefficient, $(p^*-p_s^*)/\frac{1}{2}\rho_L^*u_s^{*2}$	Re　Reynolds number, $\rho_L^*u_s^*R_s^*/\mu_E^*$
D　distance between bubbles	S*　surface tension of the liquid
k　polytropic index for the gas inside the bubbles	t　dimensionless time, $t^*u_s^*/R_s^*$
p^*　fluid pressure	t　time
p_s^*　upstream pressure	u　dimensionless fluid velocity, u^*/u_s^*
p_v^*　vapor pressure	u*　fluid velocity

u_s^* upstream fluid velocity	β dimensionless radius of the Venturi throat
V volume of the bubble, $V = 4/3\pi R^3$	η dimensionless bubble population per unit liquid volume, $\eta^* R_s^{*3}$
We Weber number, $\rho_L^* u_s^{*2} R_s^* / S^*$	η^* bubble population per unit liquid volume
x* Eulerian coordinate	γ ratio of specific heats of the gas inside the bubbles
x dimensionless Eulerian coordinate, x^*/R_s^*	μ_E^* effective dynamic viscosity of the liquid
Greek Letters	ρ dimensionless fluid density
α void fraction of the bubbly fluid	ρ_L^* density of the liquid
α_c upstream void fraction at which flashing occurs	σ cavitation number, $\left(p_s^* - p_v^*\right)/1/2\,\rho_L^* u_s^2$
α_s upstream void fraction	

1   Introduction

The Venturi generally corresponds to the measurement of flow rates in single-phase flow. Its study in the case of a bubble flow makes it possible to visualize the effect of the angles converging and diverging (through the adimensional radius β of the Venturi) on the mixing parameters. Multiphase flow measuring is generally more difficult. The density of a gas-liquid mixture depends upon the volume fraction of the gas, and the phases densities. The investigations of homogeneous steady-state cavitating nozzle flows, using spherical bubble dynamics with a polytropic thermal process [1], have shown some flow instabilities illustrated by flashing flow phenomenon.

The flow model, a generally used, is a nonlinear continuum bubbly mixture which is coupled with the dynamics equation of the bubble. A three equations model was first proposed by van Wijngaarden [2 ,3] and has been used for studying steady and transient shock wave propagation in bubbly liquids, by omitting the acceleration of the mean flow. This model has been also considered by Wang and Brennen [1], in the case of converging-diverging nozzle, with an upstream variable void fraction. It was observed that significant change of the flow characteristics depends strongly on the latter and a critical bubbles radius have been obtained. Considering the gas nucleation rate, as a source term in the mass conservation equation of the bubbles, Delale et al [4] have used the previous model for the same converging-diverging nozzle. They have concluded that the encountered flow instability can be stabilised by thermal damping. Several authors have also considered the bubble dynamics equation under an appropriate form to the choose example. Among these, Wang and Brennen [5] have written it in time and radial coordinate, for a bubbly mixture, where the shock wave have been studied for spherical cloud of cavitating bubbles. Besides effect of the shocks on the bubbles interactions have been also analysed. The same Rayleigh-Plesset equation has been used by Gaston et al [6] by modelling the bubble as a potential source. The stream function has been written in function of spatial coordinate and the source term. They have analysed the effect of complex interactions through a Venturi. By introducing liquid quantity and motion equation in a spatial Rayleigh-Plesset dynamics relation, Moholkar and Pandit [7] have obtained a global dynamic equation witch have been resolved by in a three steps method. In their work they have studied the effect of the downstream pressure, the Venturi pipe ratio, the initial bubble size an the upstream void fraction, on the dynamics of the flow. Considering a one bubble motion in a Venturi, Soubiran and Sherwood [8] have obtained a dynamic equation of the flow, based on the, acting different force.

A. Ooi and R. Manasseh [9] have studied coupling effects on acoustic signature from non-linear oscillations of a group of micro bubbles by the use of Rayleigh-Plesset equation, where bubbles number and their natural frequency are significantly dependant.

More recently, Ashrafizadeh and Ghassemi [10] have experimentally and numerically investigate the effect of the geometrical parameters, such as throat diameter, throat length, and diffuser angle, on the mass flow rate, critical pressure ratio and application rang of small-sized cavitating venturi (CVs). The obtained results show that the CVs in very small size are also capable in controlling and regulating the mass flow rate while their characteristic curves are similar to those of ordinary CVs with larger throat sizes. Also, by decreasing the throat diameter of CVs, the choked mode region, critical pressure and discharge coefficient decrease. By decreasing the diffuser angle from 15 to 5 degrees in the numerical simulations, the critical pressure ratio increases and the discharge coefficient remains constant. By increasing the throat length of CVs, the critical pressure ratio decrease while discharge coefficient does not shown any changes.

Also, a variable area cavitating venturi was designed and investigated experimentally by Tian et al [11]. Four sets of experiments were conducted to investigate the effect of the pintle stroke, the upstream pressure and downstream pressure as well as the dynamic motion of the pintle on the performance of the variable area cavitating venturi. The obtained results verify that the mass flow rate is independent of the downstream pressure when the downstream pressure ration is less about 0.8. The mass flow rate is linearly dependent on the pintle stroke and increases with the upstream pressure. The discharge coefficient is a function of the pintle stroke; however it is independent of the upstream pressure. They concluded that the variable area cavitating venturi can control and measure the mass flow rate dynamically.

Zamoum and Kessal [12] have numerically investigate the dynamical of a bubbly flows in a transversal varying section duct (Venturi). The mass and momentum phases equations, which are coupled with the Rayleigh-Plesset equation of the bubbles dynamics are used. The effects of the throat dimension and the upstream void fraction on flow parameters are investigated. The numerical resolution of the previous equations set let us found that the characteristics of the flow change dramatically with upstream void fraction. Two different flow regimes are obtained: a quasi-steady and quasi-unsteady regime. The former is characterized by large spatial fluctuations downstream of the throat, which are induced by the pulsations of the cavitation bubbles. The quasi-unsteady regime corresponds to flashing flow in which occurs a bifurcation at the flow transition between these regimes.

The present work considers new modele of bubbly cavitating flow. This modele is composed by mass and momentum equation coupled with the dynamic equation of N bubbles. The Rayleigh-Plesset equation for a system of equally sized bubbles at the same distance from each other was derived. The effects of upstream void fraction, bubbles number and distance between bubbles on the bubble radius oscillation after passing the Venturi are investigated.

2   Basic Equation

The liquid is assumed to be incompressible and the interaction liquid duct wall is neglected. The total upstream bubbles population is uniform without coalescence, and the relative motion between the phases ignored. Gas and vapour densities are neglected in comparison to one of the liquid. The bubbles are assumed to have the same initial radius R_s and external friction is neglected.

Then the mixture density can be expressed in function of bubble populationη:

$$\rho = \rho_L (1 - \eta V)$$

Where $V = 4/3\,\pi R^3(x,t)$ is the volume of the bubble.

The dynamics of the bubbles can be modelled by the Rayleigh-Plesset equation [9]

$$\rho_L^* \left[R^* \frac{d^2 R}{dt^{*2}} + \frac{3}{2}\left(\frac{dR^*}{dt^*} \right)^2 \right] + \frac{4\mu_E^*}{R^*}\frac{dR^*}{dt^*} = \left(p_s^* - p_v^* + \frac{2S^*}{R_s^*} \right)\left(\frac{R_s^*}{R^*} \right)^{3k} - p^* + p_v^* - \frac{2S^*}{R^*} - p_{ext}^* \quad (1)$$

Where $R^*(t)$ is the instantaneous bubble radius, R_s^* the upstream bubble radius, μ_E^* the effective dynamic viscosity of the liquid, ρ_L^* the density of the liquid, p_s^* the upstream pressure, p_v^* the vapor pressure, S^* the surface tension of the liquid, p^* the fluid pressure and p_{ext}^* is the imposed external pressure field, where:

$$p_{ext}^* = p_{si}^* + p_{A,i}(t) \quad (2)$$

Where

$$p_{si}^* = \sum_{j \neq 1}^{Nbub} \frac{\rho_L^*}{s_{ij}} \frac{d}{dt^*}\left(R_j^{*2} \frac{dR_j^*}{dt^*} \right) \text{ is the pressure scattered by the other bubbles.}$$

Where $s_{ij} = s_{ji}$ is the distance of bubble i from bubble j, $p_{A,i}(t)$ the applied pressure of any external field on bubble i.

Combining equations (1) and (2) gives the following coupled governing equation for coupled bubble oscillations,

$$\rho_L^* \left[R^* \frac{d^2 R}{dt^{*2}} + \frac{3}{2}\left(\frac{dR^*}{dt^*} \right)^2 \right] + \frac{4\mu_E^*}{R^*}\frac{dR^*}{dt^*} = \left(p_s^* - p_v^* + \frac{2S^*}{R_s^*} \right)\left(\frac{R_s^*}{R^*} \right)^{3k} - p^* + p_v^* - \frac{2S^*}{R^*}$$
$$- \sum_{j \neq 1}^{Nbub} \frac{\rho_L^*}{s_{ij}} \frac{d}{dt^*}\left(R_j^{*2} \frac{dR_j^*}{dt^*} \right) - P_{A,i}^*\left(t^* \right) \quad (3)$$

We assume that $s_{ij} = D =$ constant. Thus the distance of any bubble to any other bubble in the bubble population is constant. We further assume that the same external driving pressure field acts on all the bubbles, that is, $P_{A,1}(t^*) = P_{A,2}(t^*) = P_{A,3}(t^*) = P_{A,4}(t^*) = P_A(t^*)$, then $R_i^*(t^*) = R_j^*(t^*) = R^*(t^*)$.

Substituting into equation (3) yields:

$$\rho_L^* \left[R^* \frac{d^2 R}{dt^{*2}} + \frac{3}{2}\left(\frac{dR^*}{dt^*} \right)^2 \right] + \frac{4\mu_E^*}{R^*}\frac{dR^*}{dt^*} = \left(p_s^* - p_v^* + \frac{2S^*}{R_s^*} \right)\left(\frac{R_s^*}{R^*} \right)^{3k} - p^* + p_v^* - \frac{2S^*}{R^*}$$
$$- \left(N_{bub} - 1 \right)\frac{\rho_L^*}{D}\left(R^{*2} \frac{d^2 R^*}{dt^{*2}} \right) - \left(N_{bub} - 1 \right)\frac{2\rho_L^*}{D}\left(R^*\left(\frac{dR^*}{dt^*} \right)^2 \right) - P_A^*\left(t^* \right) \quad (4)$$

Equation (4) represents the idealized case where all the bubbles are equally spaced, have the same initial conditions.
The non-dimensional form equation (4) is giving by:

$$R\frac{D^2R}{Dt^2}+\frac{3}{2}\left(\frac{DR}{Dt}\right)^2+\frac{\sigma}{2}\left(1-R^{-3k}\right)+\frac{4}{Re}\frac{1}{R}\frac{DR}{Dt}+\frac{2}{We}\left(R^{-1}-R^{-3k}\right)+\frac{1}{2}Cp$$

$$+\left(N_{bub}-1\right)\frac{R_s^*u_s^{*2}}{D}R^2\frac{D^2R}{Dt^2}+\left(N_{bub}-1\right)\frac{2R_s^*u_s^{*2}}{D}R\left(\frac{DR}{Dt}\right)^2+P_A=0 \tag{5}$$

Where $D/Dt=\partial/\partial t+u\partial/\partial x$ is the Lagrangian derivative, $\sigma=\left(p_s^*-p_v^*\right)/1/2\rho_L^*u_s^2$ is the cavitation number, p_v^* is the partial pressure of vapor inside the bubble. $Re=\rho_L^*u_s^*R_s^*/\mu_E^*$ is the Reynolds number, μ_E^* is the effective viscosity of liquid. $We=\rho_L^*u_s^{*2}R_s^*/S^*$ is the Weber number, S^* is the liquid surface tension and ρ_L^* is the liquid density.

Continuity and momentum equations of the bubbly flow (Wang and Brennen 1998) [1] are:

$$\frac{\partial}{\partial t}\left[(1-\alpha)A\right]+\frac{\partial}{\partial x}\left[(1-\alpha)uA\right]=0 \tag{6}$$

$$\frac{\partial u}{\partial t}+u\frac{\partial u}{\partial x}=-\frac{1}{2(1-\alpha)}\frac{\partial Cp}{\partial x} \tag{7}$$

Where $\alpha(x,t)=4/3\pi\eta R^3/\left[1+4/3\pi\eta R^3\right]$ is the bubble void fraction, $u(x,\ t)$ the fluid velocity. $Cp(x,t)=\left(p^*(x,t)-p_s^*\right)/1/2\rho_L^*u_s^{*2}$ the fluid pressure coefficient, $p(x,\ t)$ the fluid pressure, p_s^* the upstream fluid pressure, and u_s^* is the upstream fluid velocity.

Equations (5), (6) and (7) constitutes a simple model of one-dimensional flowing bubbles fluid with nonlinear bubbles dynamics.

2.1. Steady-State Solutions

Assuming steady-state conditions, all the partial time derivative terms in equations (5),(6) and (7) disappear. Then, the former equation set is transformed into an ordinary differential equation set, with only one independent variable (x):

$$(1-\alpha)uA=(1-\alpha_s)=constant \tag{8}$$

$$u\frac{du}{dx}=-\frac{1}{2(1-\alpha)}\frac{dCp}{dx} \tag{9}$$

$$R\left(u^2\frac{d^2R}{dx^2}+u\frac{du}{dx}\frac{dR}{dx}\right)\times\left(1+\frac{(N-1)}{D}R_su_s^2R\right)+\frac{3u^2}{2}\left(\frac{dR}{dx}\right)^2+2\frac{(N-1)}{D}R_su_s^2Ru^2\left(\frac{dR}{dx}\right)^2+$$

$$\frac{4}{Re}\frac{u}{R}\frac{dR}{dx}+\frac{2}{We}\left(\frac{1}{R}-\frac{1}{R^{3k}}\right)+\frac{\sigma}{2}\left(1-\frac{1}{R^{3k}}\right)+\frac{1}{2}Cp=0 \tag{10}$$

The corresponding initial conditions are:

$$R(x=0)=1,\ U(x=0)=1,\ Cp(x=0)=0$$

And the axial variation of the cross sectional takes the following from:

$$A(x) = \begin{cases} 1 & 0 < x < x_1 \\ 1 - \dfrac{(x - x_1)(1 - \beta)}{x_2 - x_1} & x_1 < x < x_2 \\ \beta & x_2 < x < x_3 \\ 1 - \dfrac{(x_4 - x)(1 - \beta)}{x_4 - x_3} & x_3 < x < x_4 \\ 1 & x_4 < x < x_5 \end{cases} \qquad (11)$$

Where β is the dimensionless radius of the Venturi throat and x the distance along the axis. In the present work it is assumed: $\beta=0.5$, $x_1=3.0$, $x_2=5.7$, $x_3=6.7$, $x_4=10.5$. This corresponds to an ISO standard Venturi (British Standards Institution) with a 21° converging section and 15° diverging section.
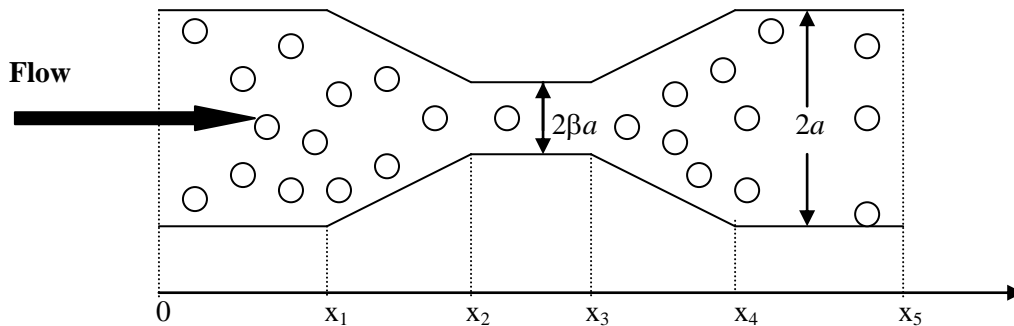

Fig. 1 Bubbly flow through a Venturi

3   Results and Discussion

Equation set (8)-(9) and (10) is resolved by the use of a fourth order Runge-Kutta scheme, with some flow conditions (Table 1).

Initial parameters	Water characteristics at 20°C
$R_s^* = 100\mu m$	$\rho_L^* = 1000 kg/m^3$
$u_s^* = 10 m/s$	$\mu_E^* = 0.03 Ns/m^2$
k=1.4	$\mu_L^* = 0.001 Ns/m^2$
Re=33	$S^* = 0.073 N/m$
$\sigma = 0.8$	
We=137	

Table1. Initial condition flow and water characteristics

Bubble void fraction effect

Five different upstream void fractions (α_s) are used in the computation to study the effect of the upstream void fraction on the flow structure through the Ventuti. The case of $\alpha_s = 0$ corresponds to the

incompressible pure liquid flow, the results are shown in Figures 2 which correspond to the non-dimensional bubble radius distribution for both cases one bubble (N=1) and two bubbles (N=2). An instability inception can be remarked in this figure for both cases, which is located just after the throat of the Venturi.

Figure 2 shown that the bubble size reach the maximum after passing the nozzle throat of the venturi with increase in the upstream void fraction, the maximum size of the bubbles increases and bubble frequency oscillation decrease, this maximum size is shifted further downstream after it reach the critical radius (instability occurs), the bubbles growth without bound in the calculation, this instability occurs when the bubble radius reaches a critical value R_c, also the void fraction growing leads to large amplitudes of the bubble radius. It can be observed that, for the case of one bubble, the instability occurs for an upstream void fraction $\alpha_s = 5.37 \times 10^{-3}$, which corresponds to a critical bubble radius $r_c = 4$. whereas, for bubble number N=2, the same phenomenon occurs for $\alpha_s = 1,344 \times 10^{-1}$, with $R_c = 1.5$. This difference is due to the bubble interaction. In the practice r_c correspond the flashing flow inception, which is illustrated by an instability of the parameters flow. The analytical expression for R_c is obtained by Wang and Brennen (1998), $R_c \approx (\sigma/2\alpha_c)^{1/3}$, where α_c is the upstream void fraction at which flashing flow occurs.
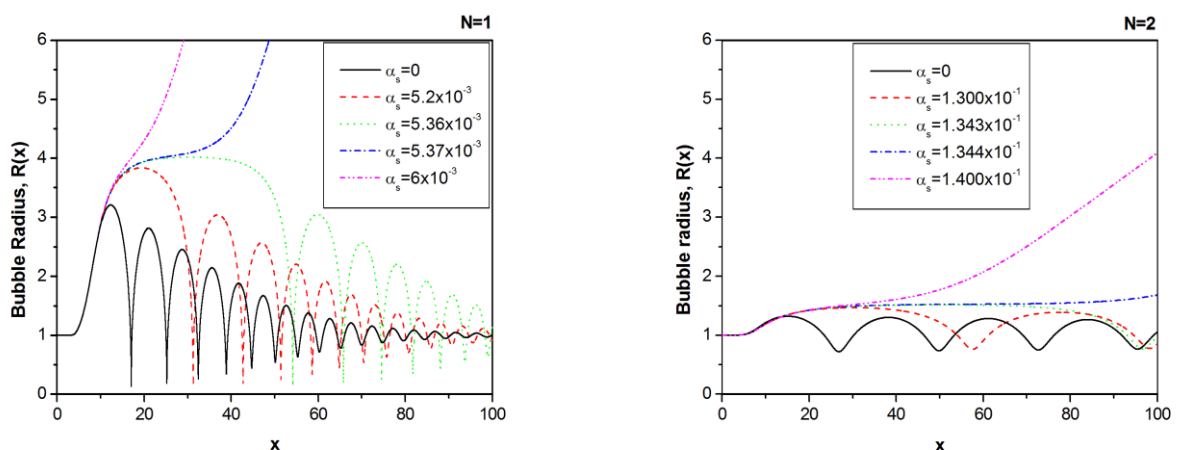

Fig. 2. Bubble radius distribution as a function of position in the flow for different upstream void fractions. $\alpha_s = 0$ correspond to the solution of the Rayleigh-Plesset equation. Dimensionless radius of the Venturi throat $\beta = 0.5$. For the case N=2, the distance between two bubbles $D = 5R_s = 500\mu m$

Bubble number effect

The effect of the presence of more than one bubble is showed in figures 3. This figure shows the non-dimensional bubble radius distribution as a function of position in the flow for bubbles number N=1, N=2 and N=3, with upstream void fraction $\alpha_s = 1 \times 10^{-3}$. The distance between bubbles for the cases N=2 and N=3 is $D = 5R_s = 500\mu m$. It can be observed here that the increasing of the bubbles number leads to decreases of the bubble oscillation frequency and the damping of the signal.
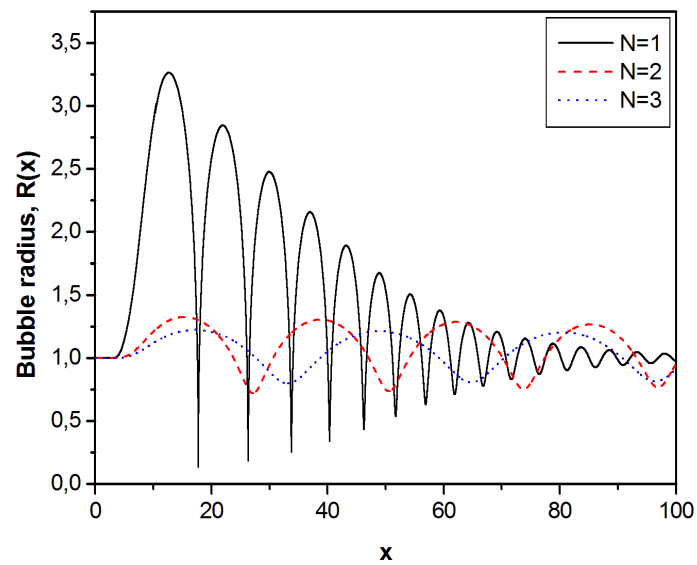
Fig. 3. Bubble radius distributions as a function of position in the flow for different bubble number. Distance between bubbles $D=5R_s=500\mu m$. Upstream void fraction $\alpha_s=1x10^{-3}$

Distance between two bubble effects

The figure 4 shows the effect of distance between bubbles on the bubbles oscillations radius. The increase distance between bubbles has an important effect on the damping radius and frequency oscillations. However; for very large distances between bubbles, the radius distribution is similar for those of one bubbles evolution.
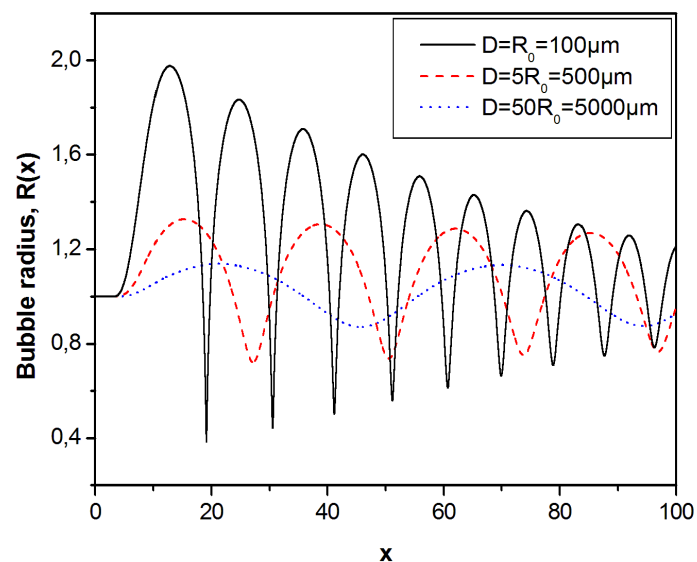

Fig. 4. Bubble radius distribution as a function of position in the flow for various values of distance between two bubbles (N=2).

3   Conclusion

A new modele mass and momentum equation coupled with the Rayleigh-Plesset equation for a system of equally sized bubbles at the same distance from each other was derived, and is validated for the case small size distance between bubbles. The effects of upstream void fraction, bubbles number and distance between bubbles are investigated. The numerical resolution of the equations set (ODE) found that the bubble radius change dramatically with upstream void fraction and an instability appeared just after the throat of the Venturi for both cases one bubble (N=1) and two bubbles (N=2). Indeed, for the case of one bubble, the instability occurs for an upstream void fraction α_s=5.37x10^{-3}, which corresponds to a critical bubble radius R_c=4. Whereas, for bubble number N=2, the same phenomenon occurs for α_s = 1,344x10^{-1}, with R_c=1.5. Also, the result found that the natural frequency and the damping of the bubbles system decrease as the number of bubbles increase. Otherwise, the increase distance between bubbles has an important effect on the damping radius and frequency oscillations. However; for very large distances between bubbles, the radius distribution is similar for those of one bubbles evolution.

References

[1] Wang, Y.-C and Brennen, C. E. One-Dimensional Bubbly Cavitating Flows Through a Converging-Diverging Nozzle. Journal of Fluids Engineering, 120, 166-170, 1998

[2] van Wijngaarden, L. One the equations of motion for mixtures of liquid and gas bubbles.   Journal of fluid mechanics, 33, 465-474, 1968

[3] van Wijngaarden, L. One-dimensional flow of liquids containing small gas bubbles. *Annual review of fluid mechanics*, 4, 369-396, 1972

[4] Delale, C. F., Kohei Okita and Yoichiro Matsumoto. Steady-State cavitating nozzle flows with nucleation. Fifth international symposium on cavitation. Osaka, Japan, November 1-4, 2003.

[5] Wang, Y.-C and Brennen, C. E. Numerical computation of shock waves in a spherical bubble cloud of cavitation bubbles. *Journal of Fluids Engineering*, 121, 872-880,1999

[6] Gaston, M. J., Reizes, J. A., Evans, G. M. Modelling of bubble dynamics in a Venturi flow with a potential flow method. *Chemical Engineering Sciences*, 65, 6427-6435, 2001

[7] Moholkar, V. S., and Pandit, A.B. Numerical investigations in the behaviour of one-dimensional bubbly flow in hydrodynamic cavitation. *Chemical Engineering Science*, 56, 1411-1418, 2001

[8] Soubiran, J. and Sherwood, J. D. Bubble motion in a potential flow within a Venturi . *journal of multiphase flow*, 26, 1771-1796, 2000

[9] Ooi. A and Manasseh. R. Coupled nonlinear oscillations of microbubbles.AZIAM. J. 46(E). pp C102_C116, 2005

[10] Ashrafizadeh SM, Ghassemi H . Experimental and numerical investigation on the performance of small-sized cavitating venturi. Flow measurement and Instrumentation, 42: 6-15, 2015

[11] Tian H, Zeng P, Yu N, Cai G. Application of variable area cavitating venturi as a dynamic flow controller. 38: 21-26, 2014

[12] Zamoum. M and Kessal. M. Analysis of cavitating flow through a Venturi. Scientific Research and Essays. Vol 10 (11) pp 367-375, 2015.